



Kahramanmaraş Sutcu Imam University Journal of Engineering Sciences



Geliş Tarihi : 19.07.2025
Kabul Tarihi : 25.12.2025

Received Date : 19.07.2025
Accepted Date : 25.12.2025

EXPERIMENTAL ANALYSIS OF PRESSURE DROP AND PUMP POWER IN PERISTALTIC PUMP-DRIVEN FLOW THROUGH FLEXIBLE PIPES OF VARYING DIAMETERS

FARKLI ÇAPLARDAKİ ESNEK BORULARDAN GEÇEN PERİSTALTİK POMPA İLE TAHRİKLİ AKIŞTA BASINÇ DÜŞÜŞÜ VE POMPA GÜCÜNÜN DENEYSEL ANALİZİ

Orhan YILDIRIM¹ (ORCID: 0000-0001-8780-1297)

¹ Atatürk University, Department of Mechanical Engineering, Erzurum, Turkey

*Sorumlu Yazar / Corresponding Author: Orhan YILDIRIM, orhanyildirim@atauni.edu.tr

ABSTRACT

Although peristaltic pumps are common in biomedical, complex fluid-structure interactions within small flexible tubes are often oversimplified by standard hydraulic theories. This study experimentally investigates the hemodynamic performance of a peristaltic pump using flexible silicone tubes with different inner diameters (6-10 mm) and wall thicknesses. Unlike traditional parametric studies, a comprehensive dimensionless analysis was conducted using the Buckingham Pi theorem to evaluate the Flow Coefficient, Head Coefficient, and Power Coefficient as functions of the Reynolds number. Additionally, Wall Shear Stress was analyzed to assess hemocompatibility. While the 10 mm tube exhibited stable hydraulic behavior, the 6 mm tube suffered from significant volumetric loss and pressure fluctuations due to radial expansion. Most critically, the dimensionless Power Coefficient in the 6 mm tube was approximately 30 times higher than in the 10 mm tube, indicating that a massive portion of hydraulic energy is dissipated to overcome wall deformation and high frictional resistance. Furthermore, WSS analysis showed that the 6 mm tube generated shear stresses reaching 90 Pa, far exceeding the physiological safety limit for hemolysis (15 Pa), whereas the 10 mm tube remained within the safe range (4–14 Pa). Pressure generation requires optimizing trade-offs with efficiency and hemocompatibility.

Keywords: Peristaltic pump, dimensionless analysis, viscoelastic deformation, wall shear stress, hemodynamics

ÖZET

Peristaltik pompalar biyomedikal uygulamalarda yaygın olarak kullanılmasına rağmen, küçük çaplı esnek borular içindeki karmaşık akışkan-yapı etkileşimi, standart hidrolik teoriler tarafından sıklıkla basite indirgenmektedir. Bu çalışma, farklı iç çaplara (6-10 mm) ve et kalınlıklarına sahip esnek silikon borular kullanarak bir peristaltik pompanın hemodinamik performansını deneysel olarak incelemektedir. Geleneksel parametrik çalışmaların aksine; Debi Katsayısı, Basınç Katsayısı ve Güç Katsayısını Reynolds sayısının fonksiyonu olarak değerlendirmek amacıyla Buckingham Pi teoremi kullanılarak kapsamlı bir boyutsuz analiz gerçekleştirilmiştir. Ayrıca, kan uyumluluğunu değerlendirmek için Duvar Kayma Gerilmesi analiz edilmiştir. 10 mm boru kararlı bir hidrolik davranış sergilerken; 6 mm boru, radyal genişleme (balonlaşma) etkisiyle önemli hacimsel kayıplara ve basınç dalgalanmalarına maruz kalmıştır. En kritik bulgu olarak; 6 mm borudaki boyutsuz güç katsayısının 10 mm boruya göre yaklaşık 30 kat daha yüksek olduğu görülmüştür. Bu durum, hidrolik enerjinin büyük bir kısmının akışkan transferinden ziyade, duvar deformasyonunu ve yüksek sürtünme direncini yenmek için harcadığını göstermektedir. Dahası WSS analizi; 10 mm borunun güvenli aralıkta (4–14 Pa) kalmasına karşın, 6 mm borunun hemoliz için fizyolojik güvenlik sınırını (15 Pa) büyük ölçüde aşarak 90 Pa seviyesine ulaşan kayma gerilmeleri oluşturduğunu göstermiştir. Basınç üretimi; verimlilik ve hemouyumluluk arasındaki ödünleşmelerin optimize edilmesini gerektirir.

Anahtar Kelimeler: Peristaltik pompa, boyutsuz analiz, viskoelastik deformasyon, duvar kayma gerilmesi, hemodinamik

INTRODUCTION

Fluid transport in flexible tubes is a critical area of research in many engineering applications. Parameters such as tube diameter, wall material, fluid properties, and flow regime directly affect system performance, influencing pressure drop, volumetric flow rate, and energy consumption. In sensitive applications—such as biomedical systems, industrial fluid transport, and chemical processes—understanding and controlling these parameters is of great importance. In this context, flow systems driven by peristaltic pumps exhibit mechanical behavior similar to the cardiovascular system, making them particularly valuable in biomedical and clinical applications.

Peristaltic pumps transport fluids by rhythmically compressing and releasing flexible tubing, allowing control over output pressure and volumetric flow rate through frequency adjustment. The relationship between frequency and flow characteristics is nonlinear and exhibits an optimum point. While increasing frequency typically raises pressure and flow at lower levels, exceeding the optimal frequency may lead to performance loss due to mechanical constraints and tube material properties (Mao et al., 2018; Banejad et al., 2020; Hostettler et al., 2023), especially in small-diameter tubing.

Pressure drop in flexible tubing is highly dependent on diameter and internal surface characteristics. Smaller diameters cause greater frictional resistance at the same volumetric flow rate, leading to increased pressure drop. This effect is further amplified by surface roughness or corrugated geometries (Dzarma et al., 2020; Santana et al., 2020). In corrugated tubes, protrusions and indentations enhance turbulence and pressure loss (Santana et al., 2020). Therefore, selecting an appropriate tube diameter is critical for energy-efficient system design.

Investigating peristaltic pump-induced flow in tubes of varying diameters is essential for modeling peristaltic motion observed in cardiovascular systems. Studies on flexible tubes with inner diameters between 6 and 10 mm are particularly relevant for biomedical modeling, as they correspond to the size range of human blood vessels. Literature reports show that increased pump frequency leads to higher pressure fluctuation amplitudes; however, exceeding the optimal frequency results in mechanical deformation and performance loss, especially in narrow tubes (Stelios et al., 2019).

Moreover, increased frequency causes a notable rise in pump power consumption, especially as tube diameter and flexibility increase. Innovative tube designs may help reduce energy use and enhance system efficiency (Manopoulos et al., 2022). While smaller diameters result in greater pressure loss due to friction, larger diameters reduce these losses and lower overall energy consumption. Experimental findings confirm that decreasing diameter increases both energy consumption and pressure drop, negatively impacting system efficiency. Additionally, as pump frequency rises, power consumption increases more significantly in larger and more flexible tubes. Advanced tube design can mitigate this effect (Manopoulos et al., 2022).

In this study, the effects of changing pump frequency on pressure behavior, volumetric flow rate, power consumption, and temporal variations in outlet pressure were experimentally investigated in flexible tubes with inner diameters of 6 and 10 mm, using a peristaltic pump. The experimental system, designed to mimic the cardiovascular system, aims to contribute to a better understanding of hemodynamic parameters and the development of more precise and efficient pumping systems for biomedical applications. As pump frequency increases, outlet pressure initially rises but then decreases after reaching an optimal point. For maximum performance and pressure, it is essential to determine the optimal frequency for the pump-tube system. Excessively high frequencies can lead to pressure loss and performance degradation, particularly in flexible tubes (Mao et al., 2018; Banejad et al., 2020; Xie et al., 2004). At high frequencies, small-diameter tubes with thin walls can undergo large-amplitude deformations, causing abrupt pressure fluctuations. Increased frequency results in more frequent compression-relaxation cycles, leading to large pressure oscillations at the inlet, especially in small, thin-walled tubes (Stelios et al., 2019).

Tube diameter has a significant influence on the hemodynamic parameters of peristaltic pump-driven flow. Experimental studies in the 6–10 mm range have shown that increasing diameter leads to higher volumetric flow

rates and greater fluid transport capacity. Since tubes in this diameter range exhibit characteristics similar to human cardiovascular structures, they are commonly preferred in biomedical research. Results also suggest that larger diameters improve pump performance stability and efficiency, although they may require better management of pressure fluctuations (Liu et al., 2024; Sánchez-Saquín et al., 2025).

This study experimentally investigates the effects of varying pump frequency on pressure characteristics, volumetric flow rate, power consumption, and transient outlet pressure in flexible tubes with diameters of 6 and 10 mm. The experimental setup, designed to resemble cardiovascular conditions, aims to enhance understanding of hemodynamic behavior and support the development of precise and efficient biomedical pumping systems.

Although the fundamental hydrodynamics of rigid pipe flows are well-established, the flow physics within peristaltic systems involving deformable boundaries present a complex Fluid-Structure Interaction (FSI) problem that cannot be fully explained by classical theories. Standard affinity laws and the Darcy-Weisbach equation often fail to predict the non-linear behavior observed in small-diameter, flexible tubes where viscoelastic wall deformation becomes a dominant energy-dissipating mechanism. Currently, there is a gap in the literature regarding how geometric scaling (specifically the interplay between tube diameter and wall thickness) affects the dimensionless hydraulic performance and hemocompatibility of these systems.

To address this gap, this study moves beyond simple parametric observations and employs a comprehensive dimensionless analysis using the Buckingham Pi theorem. By defining the Reynolds number (Re), Flow Coefficient (CQ), Head Coefficient (CH), and Power Coefficient (CP), this research aims to quantify the deviations from ideal pump theory caused by viscoelastic deformation. Furthermore, it introduces a biomedical perspective by analyzing Wall Shear Stress (WSS) to evaluate the trade-offs between hydraulic efficiency and hemolysis risk in micro-scale pumping applications.

MATERIAL AND METHOD

The primary objective of the experimental system used in this study is to establish a setup that mimics the behavior of the cardiovascular system and to analyze the effects of different stenosis geometries and pressure variations in flexible tubing on blood flow dynamics. In this context, flexible tubes with different inner diameters were examined. Flow parameters such as pressure profiles, power consumption, and volumetric flow rate were investigated in detail. The influence of tube diameter on peristaltic pump performance was comparatively evaluated. In all experiments, distilled water—exhibiting Newtonian fluid behavior—was used as the working fluid.

A schematic diagram of the experimental setup is shown in Figure 1, and its physical appearance is presented in Figure 2. After commissioning the system, calibration and validation procedures were performed to ensure accurate measurements. Subsequently, a manometer was integrated into the system to precisely monitor pressure fluctuations throughout the experiments.

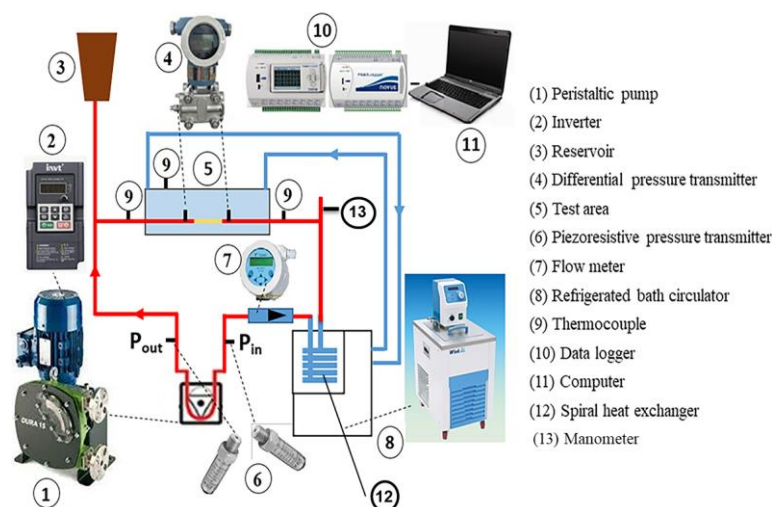


Figure 1. Schematic Diagram of the Experimental Setup and System Components (Yıldırım, 2023).

The primary components of the experimental setup were designed to operate under conditions mimicking the physiological behavior of the cardiovascular system. The test section, where flow analyses were performed, consisted of flexible silicone tubing with a total length of 30 cm. This section was located at the center of the system and served as the primary measurement zone.

To maintain the test environment at a temperature close to human body temperature, a glass water bath (15×20×45 cm) made of 4 mm thick glass was used. The system's operating temperature was set to 37 °C and kept constant throughout the experiments. The flexible tubing used to simulate vascular flow had an inner diameter of 6–10 mm, a length of 30 cm, and a Shore-A hardness range of 40–80. The physical properties of the tubing were consistent with values frequently referenced in the literature (Eslami et al., 2020; Huang et al., 2009).

Temperature control was achieved via a heat exchanger immersed in the water bath, ensuring that both the test environment and working fluid remained at a stable temperature. Pressure measurements were performed using differential pressure transmitters placed at the inlet and outlet of the test section. Additionally, a manometer was installed to monitor pressure throughout the system.

Volumetric flow rate measurements were carried out using an electromagnetic flow meter, which enabled precise real-time monitoring of the volumetric flow rate. Flow in the system was driven by a peristaltic pump, thereby generating a pulsatile flow resembling that of the cardiovascular system. Temperature, pressure, and volumetric flow rate data were collected from thermocouples, pressure sensors, and the flow meter, and transferred to a computer via a data acquisition system for digital recording.

Furthermore, piezoresistive pressure transmitters located at the inlet and outlet of the pump continuously monitored pressure fluctuations in those regions. The operating frequency of the peristaltic pump was adjusted using an inverter-supported control system, allowing for speed variation according to experimental requirements (Yıldırım, 2023; Sönmez, 2021; Sönmez et al., 2023). Only the most relevant specifications of selected key components are provided in this study.

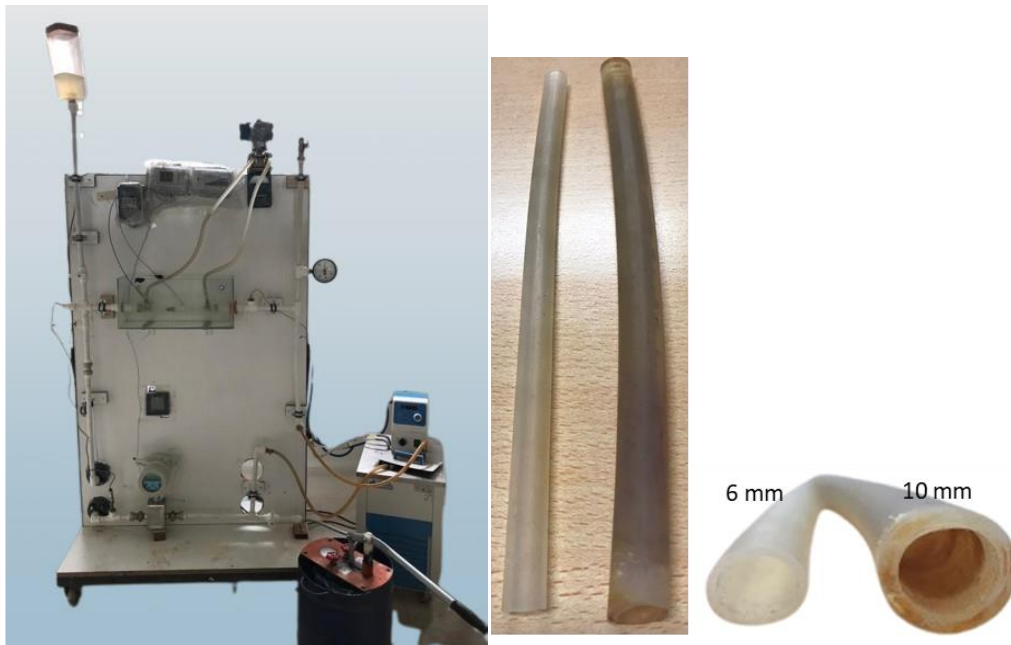


Figure 2. Image of the Experimental Setup and Flexible Silicone Tubes Used.

Silicone elastomers are widely used in various industrial and medical applications due to their favorable physical and chemical properties. These materials can operate within a broad temperature range, from –60 °C to +200 °C, and are suitable for use in environments requiring sterilization, owing to their autoclavable nature. Their high electrical insulation capacity also makes them ideal for insulation purposes in electronic components.

Table 1. Properties of the Flexible Silicone Tubes Used in the Experiments

Inner Diameter of Silicone Tube (mm)	Wall Thickness of Silicone Tube (mm)	Flexibility Level
6	1	More flexible
10	3	Less flexible

The oil-absorbing property of silicone reduces friction between surfaces, thereby minimizing wear, which presents a significant advantage from a tribological perspective. However, in terms of mechanical performance, silicone exhibits relatively low tear resistance and should therefore be used with caution in environments subjected to dynamic loads. On the other hand, its excellent resistance to aging, moisture, and ozone ensures long-lasting performance in outdoor applications. From a chemical standpoint, silicone is highly resistant to oils but not suitable for systems involving hydrocarbon solvents or steam.

Overall, silicone elastomers are reliably used in static applications and systems that require prolonged exposure to high temperatures. The Shore A hardness range typically preferred in practice is between 40 and 80, which offers an optimal balance between flexibility and mechanical strength. Considering all these properties, silicone elastomers stand out as a versatile and dependable material choice for engineering design. The image of the silicone tubes used in the study is shown in Figure 2, and their technical specifications are provided in Table 1.

**Figure 3.** Peristaltic Pump Used in the System.

The peristaltic pump evaluated in this study features a self-priming design, which enables fluid intake without the need for an external vacuum source. It is also capable of transferring fluids containing gas phases without operational issues. One of the most notable characteristics of the system is its gentle pumping action with low shear stress, making it particularly suitable for transferring biological samples or delicate fluids without causing degradation.

Another significant advantage is the pump's ability to operate under dry conditions without sustaining damage, offering enhanced operational flexibility and safety. The seal- and valve-free design minimizes leakage risks and reduces maintenance requirements. In addition, the long-lasting hose structure supports the sustainability and cost-efficiency of the pump over extended use.

From a technical perspective, the pump can achieve a maximum volumetric flow rate of 593 liters per hour and a maximum discharge pressure of 12 bar. Its suction capacity reaches up to 9.5 meters of water column. The internal diameter of the hose is 15 mm, which directly influences both the flow capacity and permeability characteristics of the pump. The maximum operating temperature the system can withstand is 80 °C. A visual representation of the pump used in this study is provided in Figure 3.

All these technical features indicate that the pump offers a compact solution with high performance, low maintenance requirements, and precise fluid transfer capabilities, even under challenging operating conditions. Peristaltic pumps of this type are widely preferred in fields such as chemistry, biotechnology, environmental engineering, and food technology due to their reliability and functional versatility.



Figure 4. Inverter Used in the Experimental Setup.

In power electronics, inverters are devices that convert electrical energy from a direct current (DC) source into alternating current (AC) with adjustable or fixed amplitude and frequency. The inverter used in the experimental setup (Figure 4) allows for direct control of the peristaltic pump's power, speed (Hz), operating frequency, and amplitude parameters. Adjustments made via the inverter directly affect pump performance, enabling precise regulation of flow conditions within the test section.

During operation, the inverter enables manual adjustment of the pump speed, thereby allowing direct control of flow-related parameters such as volumetric flow rate, outlet pressure, and pulsation characteristics. Thanks to this control structure, the system maintains high stability even under dynamic and sensitive flow conditions.

In the experimental study, all flow measurements were performed according to a predefined procedure. In the first stage, distilled water was used as the working fluid, and all components of the system were fully filled to eliminate air bubbles. The fluid level in the supply reservoir was continuously monitored throughout the experiments. Flow velocity within the system was controlled by adjusting the rotational speed of the peristaltic pump. This adjustment was made manually using a frequency-controlled inverter to simulate different pulse rates. The operating frequency range was set between 25 and 55 Hz.

The pressure values at the inlet (P_i) and outlet (P_o) of the peristaltic pump were measured using appropriately placed pressure transmitters, and the pressure difference was calculated. This difference is defined as the pressure head generated by the peristaltic pump, expressed as $\Delta P = P_i - P_o$. The system's power consumption was then calculated based on this pressure difference and the volumetric flow rate using the equation (1) below (Çengel & Cimbala, 2014):

$$\dot{W} = 2.78 \times 10^{-5} \times \dot{V} \times (P_o - P_i) \quad (1)$$

Where:

\dot{W} is the power consumed by the peristaltic pump (Watts),

\dot{V} is the volumetric flow rate (L/h),

P_i is the inlet pressure of the peristaltic pump (mbar),

P_o is the outlet pressure of the peristaltic pump (mbar).

All data were digitally recorded via a data acquisition (DAQ) system. Before each measurement, the transmitters were zeroed and the system was calibrated. To ensure measurement stability and accuracy, the system was operated for approximately 30 minutes before each experiment until steady-state conditions were achieved. Temperature was maintained at 37 °C using a hot water bath to simulate physiological conditions similar to those of the human body. Through this experimental method, the simulation of biological flow via a peristaltic pump was successfully achieved, and the flow parameters at different frequencies were evaluated in detail.

Dimensionless Analysis and Calculation of Hydraulic Parameters

To evaluate the hydraulic performance of the peristaltic pump and the flow characteristics within the flexible tubes independent of geometric scale, a dimensionless analysis was conducted. The system's governing variables were

reduced into fundamental dimensionless groups using the Buckingham Pi (π) Theorem, referencing established affinity laws for turbomachinery (Çengel & Cimbala, 2014).

Determination of Flow Regime (Reynolds Number)

While the pump rotational frequency (n) is typically used for scaling in rigid turbomachinery, it may not linearly correlate with the actual fluid velocity in small-diameter flexible tubes due to deformation and backflow effects. Therefore, to accurately characterize the flow regime (laminar vs. turbulent) and frictional behavior, the Reynolds number (Re) was determined based on the actual mean flow velocity (V) derived from the measured volumetric flow rate (Q), as shown in Equation (2):

$$Re = \frac{\rho V D}{\mu} \quad (2)$$

Here, ρ is the fluid density (kg/m^3), μ is the dynamic viscosity ($Pa \cdot s$), D is the inner diameter (m), and V is the mean velocity (m/s) calculated via the continuity equation.

Performance Parameters

To characterize the global performance of the pump system, the following dimensionless coefficients were calculated based on the pump frequency (n):

Flow Coefficient (C_Q): This represents the dimensionless volumetric flow rate transported per unit revolution of the pump (Eq.3):

$$C_Q = \frac{Q}{n D^3} \quad (3)$$

Head (Pressure) Coefficient (C_H): This parameter characterizes the dimensionless hydraulic load (pressure difference) generated by the pump (Eq.4):

$$C_H = \frac{\Delta P_{pump}}{\rho n^2 D^2} \quad (4)$$

Power Coefficient (C_P): This metric represents the dimensionless intensity of hydraulic energy required to transfer the fluid (Eq.5):

$$C_P = \frac{P_{hyd}}{\rho n^3 D^5} \quad (5)$$

Where Q is the volumetric flow rate (m^3/s), n is the pump frequency (Hz), D is the inner diameter of the tube (m), ρ is the fluid density (kg/m^3), μ is the dynamic viscosity ($Pa \cdot s$), and ΔP_{pump} is the pressure difference across the pump (Pa).

In this study, to isolate the energy costs associated specifically with fluid-structure interaction (FSI) rather than motor efficiency, the Hydraulic Power ($P_{hyd} = Q \times \Delta P_{pump}$) transferred to the fluid was used instead of electrical input power.

Wall Shear Stress (WSS) Calculation:

From a biomedical perspective, Wall Shear Stress τ_w is a critical factor in determining the risk of hemolysis in blood cells. To evaluate this, we calculated τ_w based on the momentum balance equation using the pressure drop ΔP_{tube} measured directly across the test section, as shown in Equation (6):

$$\tau_w = \frac{\Delta P_{tube} \times D}{4L} \quad (6)$$

Here, L (0.30 m) denotes the length of the flexible tube in the test section.

Uncertainty analysis

In the experimental setup, system performance data were obtained using pressure, volumetric flow rate, and temperature sensors. To evaluate the reliability of these measurements, an uncertainty analysis was conducted.

Measurement uncertainties stem from factors such as instrument selection, reading errors, observational bias, calibration sensitivity, experimental planning, and environmental conditions. This analysis provides insight into the accuracy of the experimental system and helps identify the parameters that most influence measurement deviations.

The accuracy specifications of the measurement devices used in the system are as follows:

- Temperature measurement accuracy (copper-constantan thermocouple): ±0.05%
- Pressure transmitter accuracy (test section): ±0.1%
- Piezoresistive pressure sensor accuracy: ±0.5%
- Flow meter (electromagnetic type) accuracy: ±0.2%

The overall uncertainty of the experimental system was calculated using Equation (7):

$$w_R = [(\frac{\partial R}{\partial x_1} w_1)^2 + (\frac{\partial R}{\partial x_2} w_2)^2 + \dots + (\frac{\partial R}{\partial x_n} w_n)^2]^{0.5} \tag{7}$$

where,

- w_R : total uncertainty of the system,
- R : the function of the independent variables,
- x_1, x_2, \dots, x_n : the independent variables,
- w_1, w_2, \dots, w_n : the measurement uncertainties of each independent variable

Based on this equation, the uncertainty in the calculated power consumption \dot{W} of the peristaltic pump was determined to be ±0.54% (Sönmez et al., 2023).

RESEARCH FINDINGS AND DISCUSSION

In this section, the data obtained from the experimental studies are presented and evaluated through comparison with findings reported in the literature. The effects of varying pump frequency, tube diameter, and system parameters on the performance of the peristaltic pump are discussed in detail.

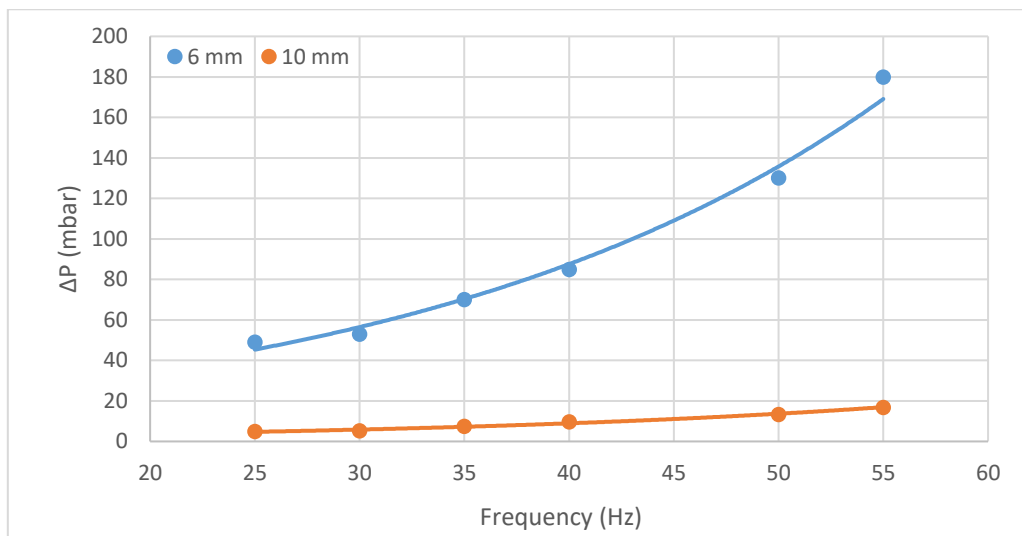


Figure 5. Effect of Frequency on Pressure Drop.

In this study, the effect of frequency variation on pressure difference (ΔP) was investigated for silicone tubes with inner diameters of 6 mm and 10 mm, as shown in Figure 5. It was observed that ΔP increased with frequency for both tube sizes (Hoskins & Lawford, 2017). At the same frequency levels, larger tube diameters resulted in lower ΔP values (Stefanadis et al., 1998; Çengel & Cimbala, 2014). This behavior can be attributed to the increased flow resistance caused by higher friction in smaller-diameter tubes.

While ΔP values were relatively close for both diameters at lower frequencies, the difference became more pronounced as frequency increased (Banerjee et al., 2003). This indicates that friction and constriction-induced resistance in smaller tubes becomes more sensitive to frequency changes. As tube diameter decreases, the fluid experiences greater frictional forces at a given volumetric flow rate, leading to a higher pressure drop. For instance, a pressure drop of 266.64 Pa was measured for a 0.5-inch diameter pipe, whereas it was only 13.33 Pa for a 1.25-inch pipe (Nuryoto et al., 2024; Cao et al., 2025; Santana et al., 2020; Shin et al., 2024). In larger-diameter tubes, reduced wall contact area lowers frictional losses and, consequently, pressure drop (Mansour et al., 2020; Chen et al., 2023). Finally, Hostettler et al. (2023) highlighted the significant influence of the tube's viscoelastic properties and diameter-to-frequency ratio on pump efficiency, noting that at higher frequencies, efficiency improves alongside deformation.

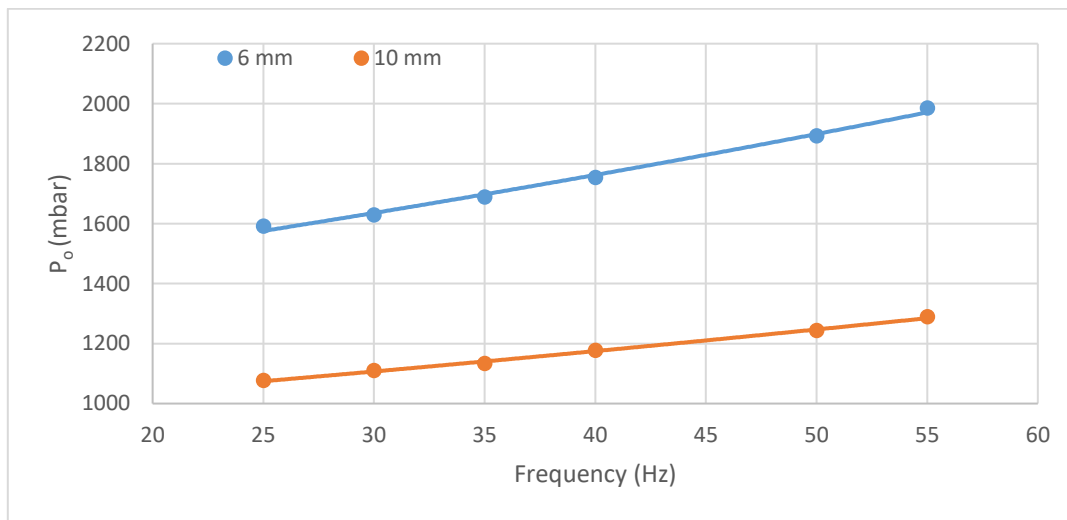


Figure 6. Effect of Frequency on Pump Outlet Pressure

In this study, the effect of frequency variation on the outlet pressure of the peristaltic pump was compared for silicone tubes with inner diameters of 6 mm and 10 mm, as illustrated in Figure 6. According to the figure, an increase in frequency led to a rise in outlet pressure for both tube diameters (Çengel & Cimbala, 2014). As frequency increases, the pump performs more frequent compressions, generally resulting in higher outlet pressure and volumetric flow rate (Mao et al., 2018; Banejad et al., 2020; Xie et al., 2004).

At higher frequencies, narrow and thin-walled tubes exhibit more pronounced pressure fluctuations and tube deformation. In contrast, these effects are more limited in larger-diameter tubes (Stelios et al., 2019). As the tube diameter increases, a decrease in outlet pressure is observed. Additionally, it has been reported that increasing arterial stenosis (transitioning from a healthy artery (0% narrowing) to one with 80% narrowing) results in a gradual increase in outlet pressure (Banerjee et al., 2003; Pandey et al., 2020). This suggests that narrowing vessel structures increase the hemodynamic load at the pump outlet.

In this study, the effect of frequency variation on the inlet pressure of a peristaltic pump was compared for silicone tubes with inner diameters of 6 mm and 10 mm, as illustrated in Figure 7. According to the experimental data, the inlet pressure of the pump tends to decrease with increasing frequency for both tube sizes (Çengel & Cimbala, 2014). Similarly, as the tube diameter increases, the reduction in inlet pressure becomes more pronounced. This can be explained by the fact that higher frequency and volumetric flow rate enhance the suction capability of the peristaltic pump, thereby reducing the inlet pressure.

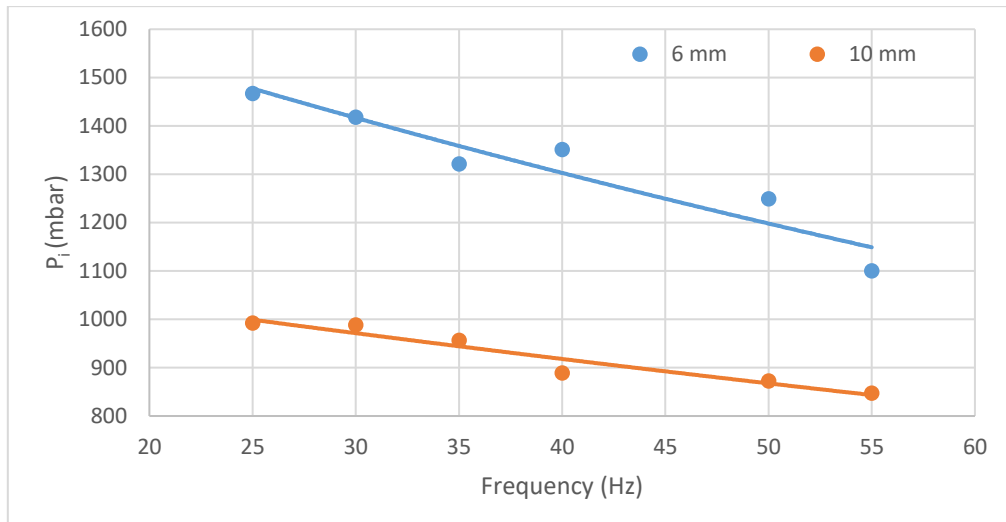


Figure 7. Effect of Frequency on Pump Inlet Pressure

As the pump frequency increases, the more frequent compression and relaxation cycles of the tube wall lead to high-amplitude fluctuations in inlet pressure. This effect is especially evident in small-diameter and thin-walled tubes, where deformation can reach up to 60% of the tube radius (Stelios et al., 2019). Additionally, as arterial stenosis increases from 0% to 80% a gradual decrease in pump inlet pressure has been reported. This indicates that under increased vascular resistance, the suction performance of the pump is reduced (Banerjee et al., 2003).

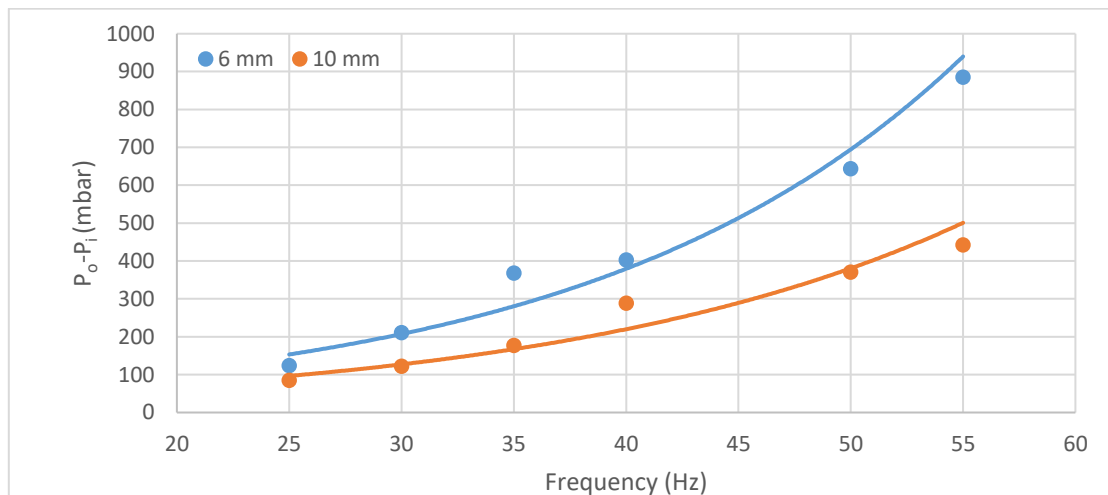


Figure 8. Effect of Frequency on Pump Pressure Difference

In this study, the effect of frequency variation on the pressure difference across the peristaltic pump ($P_o - P_i$) was investigated for silicone tubes with inner diameters of 6 mm and 10 mm, as illustrated in Figure 8. According to the experimental results, the pressure difference between the outlet and inlet of the pump increases with frequency for both tube diameters (Stefanadis et al., 1998; Çengel & Cimbala, 2014). This increase is more pronounced in small-diameter tubes, which can be attributed to higher frictional resistance requiring the pump to generate greater outlet pressure. At low frequencies, the pressure differences observed in both tube sizes are relatively similar. However, as the frequency increases, this difference becomes significantly larger (Banerjee et al., 2003). This trend indicates that increased volumetric flow rate enhances flow resistance in the system, leading to a greater pressure differential.

As frequency increases, both the pressure difference and the amplitude of pressure fluctuations grow. These effects are especially evident in small-diameter, thin-walled tubes, where increased deformation directly affects pump performance and pressure profiles. In contrast, these impacts remain limited in large-diameter, thick-walled tubes (Stelios et al., 2019). This behavior is related to the concept of hydraulic diameter: in narrow tubes, the ratio of internal surface area to flow cross-sectional area is higher, resulting in greater friction and, therefore, a higher required pressure difference. Conversely, in larger tubes, reduced resistance allows for sufficient flow with a lower pressure gradient. Additionally, a gradual increase in pump-induced pressure difference was observed as the degree of arterial

stenosis increased from 0% to 80% (Banerjee et al., 2003; Sönmez, 2021). This demonstrates that rising vascular resistance increases the load on the pump, thereby elevating the hemodynamic pressure difference.

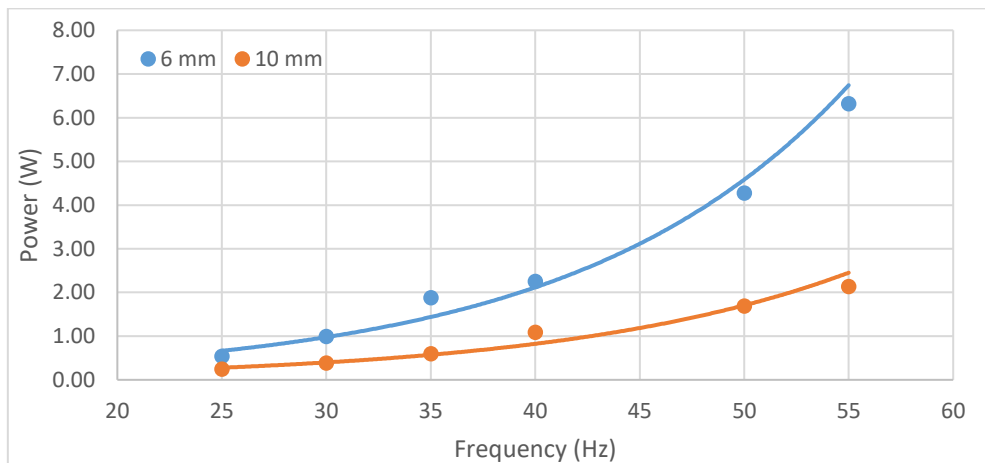


Figure 9. Effect of Frequency on Pump Power Consumption

In this study, the effect of frequency variation on the power consumption of a peristaltic pump was investigated using silicone tubes with inner diameters of 6 mm and 10 mm, as shown in Figure 9. According to the figure, the pump’s power consumption increases with rising frequency for both tube diameters (Manopoulos et al., 2022). This increase is especially significant in small-diameter tubes, where higher pressure differences induced by increased frequency result in greater energy demand (Çengel & Cimbala, 2014).

At lower frequencies, the power consumed by the pump for both 6 mm and 10 mm tubes is relatively similar. However, as the frequency increases, the difference in power consumption becomes more pronounced (Banerjee et al., 2003). This is primarily due to the higher flow resistance in smaller tubes, which forces the pump to generate more pressure. This relationship is also supported by the Darcy–Weisbach equation, which states that: $\Delta P \propto 1/D^5$. This equation illustrates that as tube diameter decreases, pressure loss increases dramatically. The resulting increase in pressure difference directly leads to higher energy consumption by the pump. From an energy efficiency perspective, the 10 mm diameter tube can be considered more advantageous, as it offers lower flow resistance and less structural deformation under the same operating conditions.

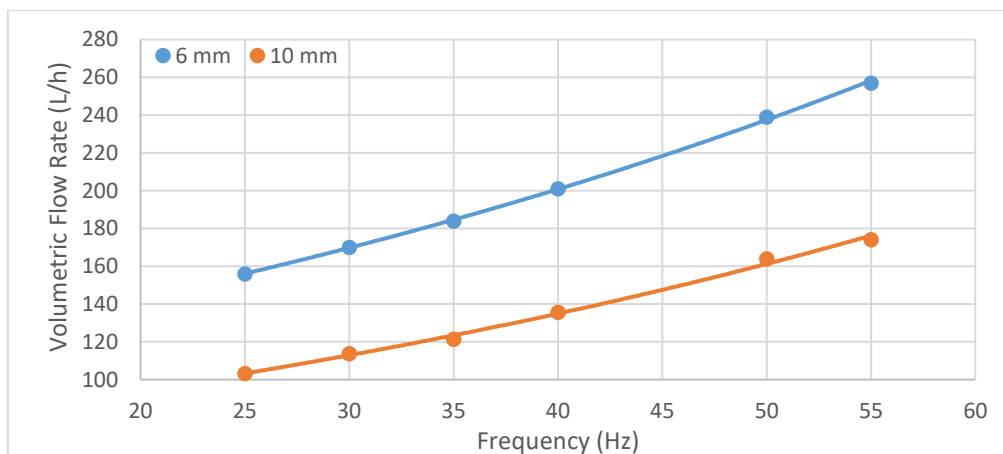


Figure 10. Effect of Frequency on Volumetric Flow Rate

In this study, the effect of frequency on the volumetric flow rate was analyzed for silicone tubes with inner diameters of 6 mm and 10 mm, as shown in Figure 10. Generally, as tube diameter increases, the pump requires lower outlet pressure to maintain the same volumetric flow rate (Stefanadis et al., 1998; Çengel & Cimbala, 2014). However, the experimental results indicate that increasing frequency leads to higher outlet pressure (see Figure 6), which in turn increases the volumetric flow rate in both tube types.

Goulpeau et al. (2005) reported that volumetric flow rate increases linearly with frequency up to 250 Hz. At lower frequencies, the peristaltic pump transfers volume more frequently, thereby increasing volumetric flow rate; however, at higher frequencies, valve responsiveness becomes limited, and flow saturation occurs. The same study also noted that a working pressure of 0.6 bar yielded a higher volumetric flow rate compared to 0.2 bar.

Experimental findings indicate that frequency has a flow-enhancing effect dependent on the inner diameter of the tube (Verde et al., 2021). As frequency increases, the roller rotation count rises, resulting in greater volume transfer per unit time. In elastic silicone tubes, volumetric flow rates exceeding 250 L/h are achievable (Esser et al., 2019; Tauber et al., 2021). However, material fatigue and viscoelastic behavior at high frequencies can limit long-term flow performance (Hostettler et al., 2023).

Volumetric flow rate is primarily dependent on pump frequency and the flow resistance of the tube. Although small-diameter tubes may permit higher velocities, the Darcy–Weisbach equation ($\Delta P \propto 1/D^5$) demonstrates that pressure loss increases dramatically as diameter decreases, thereby limiting volumetric flow rate. On the other hand, laminar flow and smooth inner surfaces in narrow tubes can enhance pressure-flow efficiency (Grishin, 2020).

Hung and Lim (2015) modeled the effects of tube diameter and wall thickness on flow and deformation, showing that deformation increases with diameter; however, excessively large diameters may reduce overall system efficiency. They found that increasing the tube diameter from 2 mm to 4 mm increased the deformation and strain of soft tubes, with peak flow velocities occurring at a diameter and thickness of 4 mm and 1 mm, respectively. In the present study, the physical behavior of the tubes was governed by the wall thickness data presented in Table 1, rather than diameter alone. The 10 mm tube, with its significant 3 mm wall thickness, exhibited high structural rigidity. Therefore, contrary to the 'elastic reservoir' hypothesis, this tube resisted radial expansion. Its lower flow performance is attributed to the high mechanical resistance of the thick wall against the pump rollers, which likely prevented complete occlusion (squeezing) and reduced the effective stroke volume. In contrast, the 6 mm tube, having a wall thickness of only 1 mm, demonstrated high flexibility. The dimensionless Flow Coefficient (C_Q) analysis revealed that this thin-walled tube acted as a viscoelastic reservoir, undergoing radial deformation (ballooning) at high frequencies. Although the 6 mm tube achieved higher net volumetric flow rates due to high flow velocity and turbulence, the steep decline in its C_Q values indicates that a significant portion of the potential volumetric efficiency was lost to this wall deformation.

As observed in Figure 10, a positive correlation exists between frequency and volumetric flow rate for both diameters, though this relationship varies with tube size. In the 6 mm tube, volumetric flow rate increased significantly with frequency. In contrast, in the 10 mm tube, the volumetric flow rate increased from 100 L/h to only 175 L/h over the same frequency range. Although inlet–outlet pressure differences were not constant, it was found that outlet pressure in the 6 mm tube was notably higher. Volumetric flow rates and frequencies were measured across various flow regimes, revealing a positive correlation between frequency and volumetric flow rate for both tube sizes. However, this relationship was more pronounced in smaller tubes.

Reynolds number calculations indicated fully turbulent flow in both systems: $Re \approx 22,000$ for the 6 mm tube and $Re \approx 9000$ for the 10 mm tube at the highest frequency. These results differ significantly from the Spencer & Reid (1979) carotid artery stenosis model, which suggests that while blood velocity initially increases with narrowing diameter, volumetric flow rate begins to decline once the critical threshold (≈ 1.5 mm) is crossed due to increased vascular resistance and pressure stabilization. That model is based on laminar flow and physiological boundaries of biological systems. In contrast, in this study's experimental setup, the higher inlet pressure observed in the 6 mm tube enabled sustained or even increased flow despite the narrow diameter. The turbulent regime indicated by the Reynolds numbers suggests that the classical Poiseuille formulation does not apply. In turbulent flow, the velocity profile flattens and the friction factor decreases, allowing for higher velocities and volumetric flow rates.

Therefore, the observed increase in volumetric flow rate despite narrowing diameter is attributed to particles carrying higher kinetic energy in turbulent conditions, along with elevated inlet pressure. Since turbulence was not considered in the Spencer & Reid model, the rise in volumetric flow rate observed here does not directly align with their findings. In conclusion, the data in this study reveal that hemodynamic models may vary significantly depending on parameters such as pressure, flow regime (laminar vs. turbulent), and diameter. These findings emphasize the importance of clearly defining the flow regime and hydrodynamic boundaries, particularly when modeling arterial systems.

Another key point highlighted in Spencer & Reid's study is the reliability of Doppler frequency as an indicator, especially in severe stenosis cases ($>70\%$). In the present model, the limited increase in volumetric flow rate despite higher frequency supports the notion that approaching a critical diameter can significantly alter the flow regime.

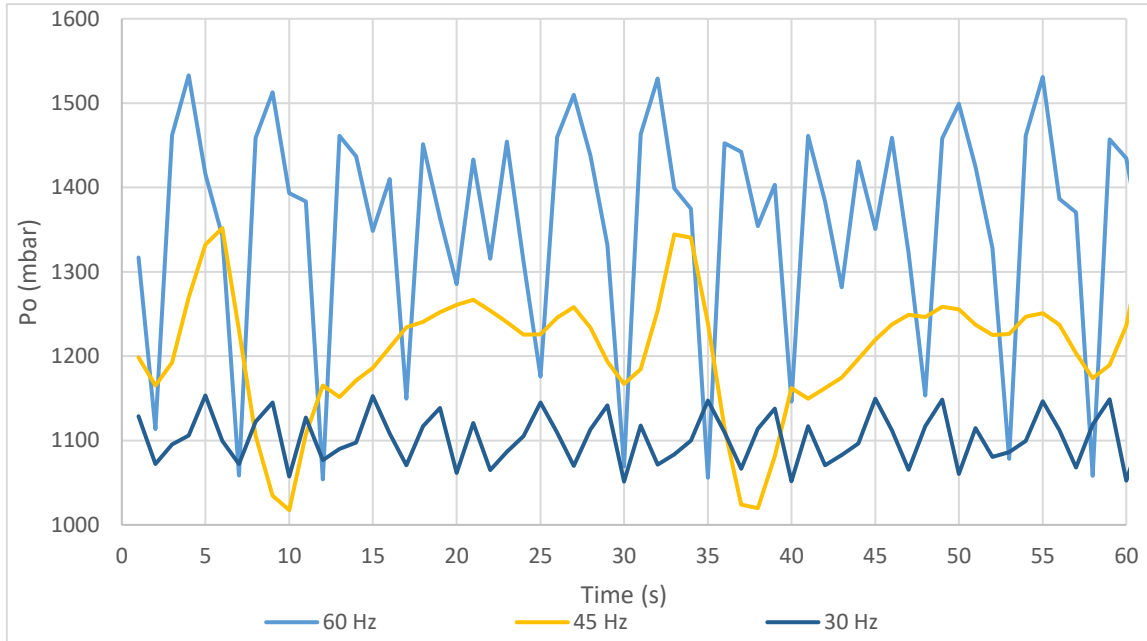


Figure 11. Temporal Variation of Outlet Pressures at Different Frequencies for the 10 mm Flexible Tube

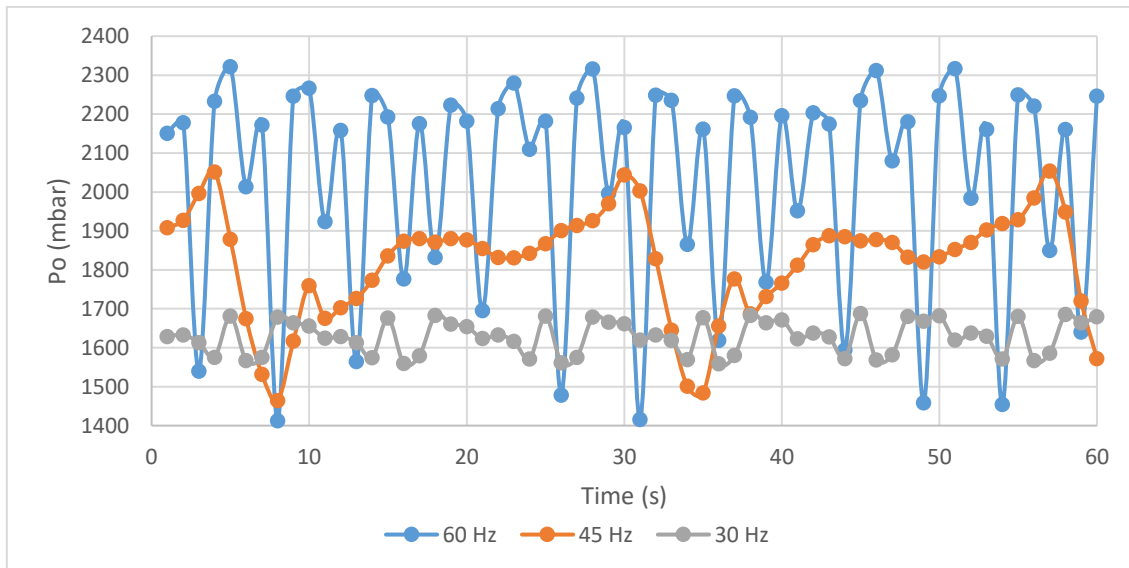


Figure 12. Temporal Variation of Outlet Pressures at Different Frequencies for the 6 mm Flexible Tube

Experimental data were analyzed to evaluate the temporal variation of outlet pressures at different frequencies for both 6 mm and 10 mm inner-diameter silicone tubes. The corresponding pressure amplitudes were also graphed (Figures 11 and 12). A comparison of the results shows that, across the tested frequencies, the 6 mm tube exhibits higher outlet pressures than the 10 mm tube. This trend is consistent with expectations, as increased pump volumetric flow rate and associated frequency lead to higher outlet pressure (Stefanadis et al., 1998; Çengel & Cimbala, 2014).

The figures also reveal that the difference between the maximum and minimum outlet pressures increases with frequency for both tube diameters, indicating higher pressure amplitude at higher frequencies. Additionally, as flow constriction increases in both tubes, both maximum and minimum outlet pressures rise accordingly.

Analysis of Dimensionless and Hydraulic Parameters

In this section, the hydraulic performance of the peristaltic pump system and the flow characteristics within the

flexible tubing are analyzed using dimensionless parameters: Reynolds number (Re), Flow Coefficient (C_Q), Head Coefficient (C_H), Power Coefficient (C_P), and Wall Shear Stress (WSS). The analysis primarily focuses on the influence of tube wall thickness and geometric scaling on deformation behavior and overall system efficiency. The analysis of the Head Coefficient (C_H), which represents the system's capacity to generate hydraulic load and its inherent resistance, is presented in Figure 13.

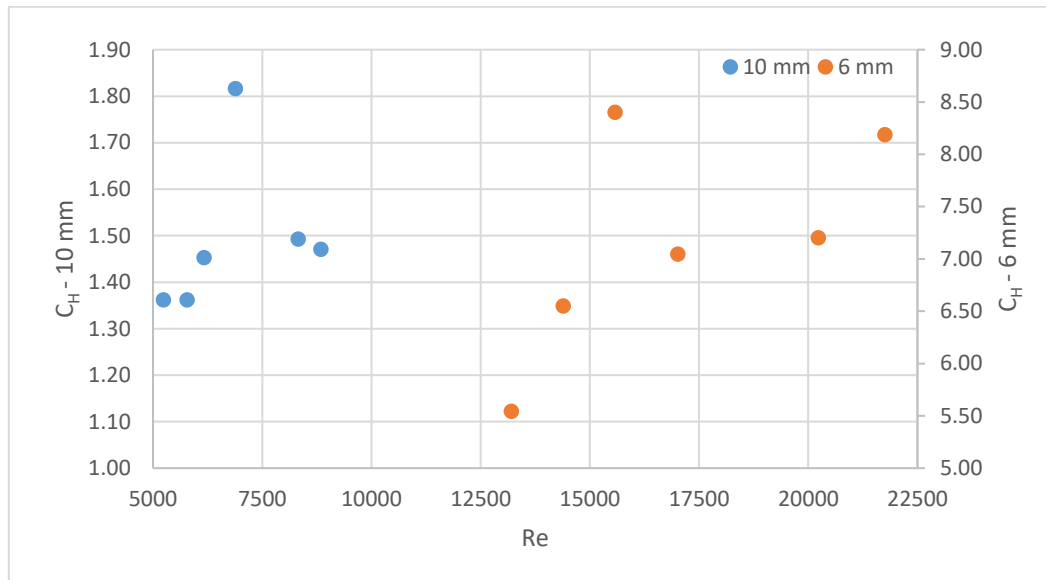


Figure 13. Comparison of Dimensionless Head Coefficient (C_H) for 6 mm and 10 mm Tubes

The results reveal that geometric scaling has a dramatic, non-linear impact on flow physics. 10 mm Tube: Flow resistance is minimal, with C_H values hovering at very low levels between 1.4 and 1.8. 6 mm Tube: Due to the constricted cross-section and increased flow velocity, viscous friction forces become dominant, causing C_H values to surge to the 5.6-8.2 range.

The approximately 6 to 7 fold difference between the 10 mm and 6 mm tubes cannot be attributed solely to the diameter effect described by the Darcy-Weisbach law ($h_f \propto 1/D^5$). The compliance of the thin-walled (1 mm) 6 mm tube absorbs energy by expanding under pressure, thereby increasing the hydraulic load the pump must generate and maximizing the system's dimensionless pressure requirement. Takagi & Balmforth (2011) stated that flow pumped by peristaltic waves in flexible pipes shows efficiency changes depending on deformation. Similarly, in this study, the effect of elastic pipes on hydraulic efficiency was evaluated together with waveform and diameter changes. The Power Coefficient (C_P) values, which indicate the system's energy efficiency and the hydraulic energy intensity required to transfer a unit of fluid, are compared in Figure 14.

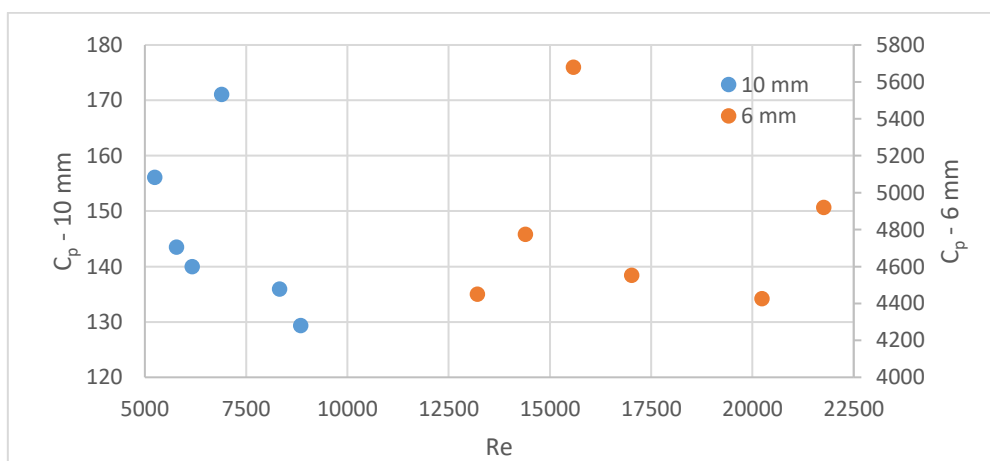


Figure 14. Variation of Dimensionless Power Coefficient (C_P) with Reynolds Number and Energy Cost Analysis

The most striking finding of this study emerges from this analysis: 10 mm Tube: C_p values remain within the 130 – 170 band. 6 mm Tube: C_p values skyrocket to the order of 4400 – 5700.

This massive discrepancy highlights a critical energy bottleneck created by small-diameter, thin-walled tubes. In the 6 mm tube, a substantial portion of the hydraulic energy is consumed not by net fluid transport, but by overcoming high friction in the narrow cross-section and the viscoelastic deformation of the tube wall (work loss). This result quantitatively demonstrates that in micro-scale or narrow-section biomedical pump designs, reducing the diameter increases the energy cost exponentially. El-Abbasi et al. (2011) showed that tube deformation in a peristaltic pump increases the energy requirements of the system and that this effect should be modeled with FSI.

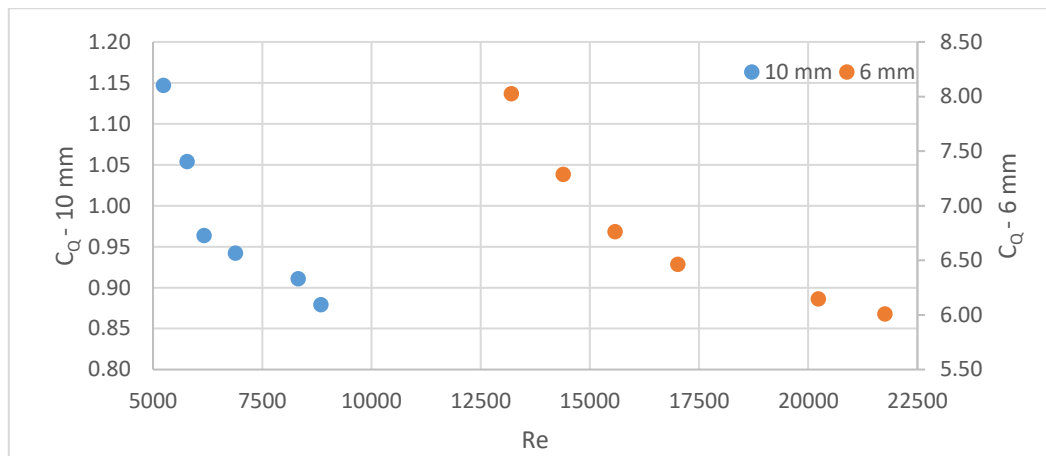


Figure 15. Variation of Flow Coefficient (C_Q) with Reynolds Number for Different Tube Diameters

Although peristaltic pumps are theoretically classified as positive displacement machines, they experience practical volumetric losses due to the deformation of flexible tubing. Figure 15 illustrates the variation of the dimensionless Flow Coefficient (C_Q) with respect to the Reynolds number. As observed in the graph, the C_Q values for both tube diameters exhibit a declining trend as the Reynolds number (and consequently, the frequency) increases. However, this decline is significantly more pronounced in the 6 mm diameter tube with a 1 mm wall thickness.

10 mm Tube (3 mm wall thickness): Thanks to its thicker wall structure, this tube maintained sufficient rigidity against high pressure, resulting in a relatively stable C_Q trajectory within the range of 1.15 – 0.88. 6 mm Tube (1 mm wall thickness): Due to its thinner wall structure, this tube suffered from significant radial expansion (compliance/ballooning effect) under pressure at high frequencies. The insufficient relaxation time required for the tube to recover its shape after compression, combined with increased backflow, caused the C_Q value to plummet sharply from 8.02 to 6.01. This finding is consistent with existing literature, confirming that thin-walled flexible tubes lose geometric stability at high frequencies, thereby compromising volumetric efficiency. Kozlovsky et al. (2015) analyzed the effects of diameter variation on net flow rate in a dimensionless analysis of valve-free peristaltic pump systems in elastic tubes. Their study emphasizes that deformation in narrow tubes causes flow rate loss.

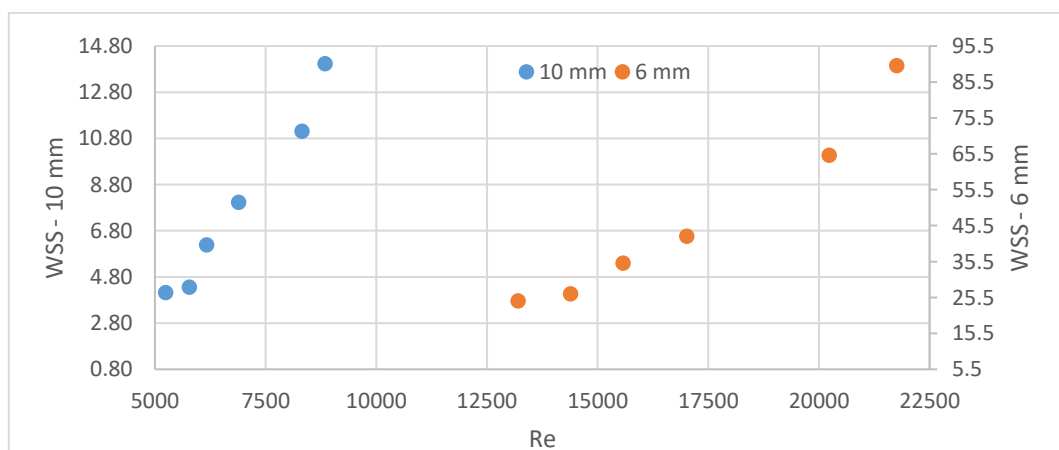


Figure 16. Variation of Wall Shear Stress Values with Reynolds Number and Evaluation of Hemolysis Risk

In cardiovascular applications, Wall Shear Stress (WSS) is a paramount parameter for preventing mechanical damage to blood cells (hemolysis). WSS values were calculated based on the measured pressure drop and are presented in Figure 16. Literature generally defines the physiological WSS range for human arteries as 1–15 Pa, noting that stresses exceeding this limit pose a risk of platelet activation and hemolysis.

- 10 mm Tube: The calculated WSS values range from 4 – 14 Pa, falling well within physiological limits and offering a safe hydrodynamic environment.
- 6 mm Tube: Due to the constricted cross-section, increased velocity, and turbulent flow regime, WSS values surge to levels of 24 – 90 Pa.

Notably, shear stresses reaching 90 Pa carry a severe risk of cellular damage during the transfer of sensitive biological fluids. This finding proves that focusing solely on volumetric flow rate targets in pump systems is insufficient; tube diameter and wall thickness selection must be optimized in accordance with WSS limits. Hung & Lim (2015) showed that the deformation and stress levels in flexible tubes in peristaltic pumps vary significantly depending on their thickness and diameter. It was particularly emphasized that surface-related parameters such as WSS are affected by such deformations.

Collectively, these dimensionless and hemodynamic analyses demonstrate that the behavior of peristaltic pumps in small-diameter flexible tubes cannot be predicted solely by standard affinity laws or geometric scaling. This study reveals a critical trade-off governed by the tube's wall thickness and compliance. While the 10 mm tube (3 mm wall thickness) offers a hydraulically stable and biologically safe transport zone, the 6 mm tube (1 mm wall thickness) presents a dual disadvantage: an exponential increase in energy cost (high C_P) and a potential risk of cellular damage (high WSS). Consequently, this research underscores that in the design of biomedical micro-pumping systems, wall thickness and viscoelastic deformation are not merely structural attributes but active hydrodynamic parameters that define the limits of both energy efficiency and hemocompatibility.

CONCLUSION

In this study, the hemodynamic parameters of flow generated by a peristaltic pump in flexible silicone tubes with different inner diameters (6 mm and 10 mm) and wall thicknesses (1 mm vs. 3 mm) were experimentally investigated. Unlike traditional performance reports, this study employed a comprehensive dimensionless analysis to reveal the underlying fluid-structure interaction (FSI) mechanisms governing the system. The analysis revealed that:

1. **Pressure and Deformation:** An increase in pump frequency results in higher pressure difference (and outlet pressure). These effects are more pronounced in the 6 mm tube, where increased frequency leads to greater pressure fluctuations. This instability is attributed to the thin-walled (1 mm) structure of the 6 mm tube, which exhibits significant radial expansion (compliance effect) compared to the more rigid, thick-walled (3 mm) 10 mm tube.
2. **Energy Efficiency (C_P Analysis):** The dimensionless Power Coefficient (C_P) analysis exposed a critical energy bottleneck. While energy consumption naturally increases with frequency, the 6 mm tube exhibited C_P values approximately 30 times higher than the 10 mm tube. This proves that in small-diameter, thin-walled tubes, a massive portion of hydraulic energy is dissipated to overcome viscoelastic wall deformation and high frictional resistance, rather than transporting the fluid. Therefore, for energy-prioritized applications, larger diameters are strictly recommended.
3. **Volumetric Efficiency (C_Q Analysis):** Volumetric flow rate analysis indicated that the Flow Coefficient (C_Q) decreases as the Reynolds number increases, contradicting the theoretical constant behavior of positive displacement pumps. This loss in volumetric efficiency is strictly associated with the viscoelastic time-response (relaxation time) of the tube material, which fails to recover its shape fast enough at high frequencies, leading to backflow and ballooning.
4. **Biomedical Implications (WSS Analysis):** A crucial trade-off was identified regarding hemocompatibility. Wall Shear Stress (WSS) analysis showed that while the 10 mm tube maintained shear stresses within the physiological safety limits (4–14 Pa), the 6 mm tube generated excessive stresses reaching up to 90 Pa due to the turbulent flow regime (20,000). This finding highlights a severe risk of hemolysis in the transport of sensitive biological fluids through small-diameter lines.

Overall, this study provides valuable reference data for the optimization of peristaltic pump-driven systems. It is concluded that tube wall thickness and viscoelastic deformation are not merely structural attributes but active hydrodynamic parameters that define the limits of both energy efficiency and hemocompatibility. Future studies should focus on long-term fatigue analysis of different viscoelastic materials under these high-shear conditions.

ACKNOWLEDGMENTS

This study was conducted in the experimental system established under project number FCD-2019-7316 by the Atatürk University Scientific Research Projects Coordination Office.

ARTIFICIAL INTELLIGENCE CONTRIBUTION STATEMENT

The language edits and textual improvements in this study were carried out using an artificial intelligence-supported tool (ChatGPT). However, the text, data analysis, figures and all scientific content were created solely by the author(s) and the scientific responsibility is assumed by the author(s).

REFERENCES

- Banejad, A., Shaegh, S. A. M., Ramezani-Fard, E., Seifi, P., & Passandideh-Fard, M. (2020). On the performance analysis of gas-actuated peristaltic micropumps. *Sensors and Actuators A: Physical*, 315, 112242. <https://doi.org/10.1016/j.sna.2020.112242>
- Banerjee, R. K., Back, L. H., & Back, M. R. (2003). Effects of diagnostic guidewire catheter presence on translesional hemodynamic measurements across significant coronary artery stenoses. *Biorheology*, 40(6), 613–635. <https://doi.org/10.1177/0006355X2003040006001>
- Cao, Y., Xu, Q., Yu, H., Li, Y., Huang, B., & Guo, L. (2025). Pressure drop of slug flow in horizontal pipes with different pipe diameters and liquid viscosities. *Physics of Fluids*, 37(2), 023341 <https://doi.org/10.1063/5.0253250>
- Cengel, A. Y., & Cimbala, J. M. (2014). *Fluid Mechanics Fundamentals and Applications (Third)*. McGraw-Hill Education.
- Chen, Y., Zhao, C., Huang, Q., Li, S., Huang, J., Ni, X., & Wang, J. (2023). Impact of Pipe Diameter on the Discharge Process of Halon1301 in a Fire Extinguishing System with Horizontal Straight Pipe. *Fire*, 6(8), 287. <https://doi.org/10.3390/fire6080287>
- Dzarma, G., Adeyemi, A., & Taj-Liad, A. (2020). Effect of inner surface roughness on pressure drop in a small diameter pipe. *International Journal of Novel Research in Engineering and Science*, 7(1), 1-8.
- El-Abbasi, N., Bergström, J. S., & Brown, S. B. (2011). Fluid-Structure Interaction Analysis of a Peristaltic Pump. In COMSOL conference in Boston
- Eslami, P., Tran, J., Jin, Z., Karady, J., Sotoodeh, R., Lu, M. T., Hoffmann, U., & Marsden, A. (2020). Effect of Wall Elasticity on Hemodynamics and Wall Shear Stress in Patient-Specific Simulations in the Coronary Arteries. *Journal of Biomechanical Engineering*, 142(2), 245031–2450310. <https://doi.org/10.1115/1.4043722>
- Esser, F., Krüger, F., Masselter, T., Speck, T. (2019). Characterization of Biomimetic Peristaltic Pumping System Based on Flexible Silicone Soft Robotic Actuators as an Alternative for Technical Pumps. In: Martinez-Hernandez, U., et al. *Biomimetic and Biohybrid Systems. Living Machines 2019. Lecture Notes in Computer Science()*, vol 11556. Springer, Cham. https://doi.org/10.1007/978-3-030-24741-6_9
- Goulpeau, J., Trouchet, D., Ajdari, A., & Tabeling, P. (2005). Experimental study and modeling of polydimethylsiloxane peristaltic micropumps. *Journal of Applied Physics*, 98(4), 044914. <https://doi.org/10.1063/1.1947893>
- Grishin, A. (2020). The application of the elastic tube with the specific cross section form in the linear peristaltic pump. *MATEC Web of Conferences*, 329, 03062. <https://doi.org/10.1051/MATECCONF/202032903062>
- Hoskins, P.R., Lawford, P.V. (2017). Atherosclerosis. In: Hoskins, P., Lawford, P., Doyle, B. (eds) *Cardiovascular Biomechanics*. Springer, Cham. https://doi.org/10.1007/978-3-319-46407-7_15

- Hostettler, M., Grüter, R., Stingelin, S., De Lorenzi, F., Fuechslin, R. M., Jacomet, C., Koll, S., Wilhelm, D., & Boiger, G. K. (2023). Modelling of Peristaltic Pumps with Respect to Viscoelastic Tube Material Properties and Fatigue Effects. *Fluids*, 8(9), 254. <https://doi.org/10.3390/fluids8090254>
- Huang, J., Lyczkowski, R. W., & Gidaspow, D. (2009). Pulsatile flow in a coronary artery using multiphase kinetic theory. *Journal of biomechanics*, 42(6), 743–754. <https://doi.org/10.1016/j.jbiomech.2009.01.038>
- Hung, N. B., & Lim, O. (2015). The study about deformation of a Peristaltic Pump using Numerical Simulation. 26(6), 652–658. <https://doi.org/10.7316/KHNES.2015.26.6.652>
- Kozlovsky, P., Rosenfeld, M., Jaffa, A. J., & Elad, D. (2015). Dimensionless analysis of valveless pumping in a thick-wall elastic tube: Application to the tubular embryonic heart. *Journal of Biomechanics*, 48(9), 1652-1661. <https://doi.org/10.1016/j.jbiomech.2015.03.001>
- Liu, F., Gong, Z., Ma, X., Zhang, Y., & Song, X. (2024). Based on the combination of fluid-solid interaction mechanism model and surrogate model for peristaltic pump performance analysis and multi-objective optimization design. *Adv. Eng. Informatics*, 62, 102675. <https://doi.org/10.1016/j.aei.2024.102675>
- Manopoulos, C., Tsoukalis, A., & Mathioulakis, D. (2022). Suppression of flow pulsations and energy consumption of a drug delivery roller pump based on a novel tube design. *Proceedings of the Institution of Mechanical Engineers, Part C: Journal of Mechanical Engineering Science*, 236(14), 7759 - 7770. <https://doi.org/10.1177/09544062221084188>
- Mansour, M., Zähringer, K., Nigam, K., Thévenin, D., & Janiga, G. (2020). Multi-objective optimization of liquid-liquid mixing in helical pipes using Genetic Algorithms coupled with Computational Fluid Dynamics. *Chemical Engineering Journal*, 391, 123570. <https://doi.org/10.1016/j.cej.2019.123570>
- Mao, G., Wu, L., Fu, Y., Chen, Z., Natani, S., Gou, Z., Ruan, X., & Qu, S. (2018). Design and Characterization of a Soft Dielectric Elastomer Peristaltic Pump Driven by Electromechanical Load. *IEEE/ASME Transactions on Mechatronics*, 23, 2132-2143. <https://doi.org/10.1109/TMECH.2018.2864252>
- Nuryoto, N., Rahmayetty, R., Rumbino, Y., Damayanti, A., & Wicakso, D. R. (2024). Observasi Penurunan Tekanan (Pressure Drop) Pada Sistem Perpipaan: Pengaruh Panjang Dan Diameter Pipa, Elbow, Dan Tee. *Jurnal Rekayasa Mesin*. <https://doi.org/10.21776/jrm.v15i2.1666>
- Pandey, R., Kumar, M., Majdoubi, J., Rahimi-Gorji, M., & Srivastav, V. K. (2020). A review study on blood in human coronary artery: Numerical approach. *Computer methods and programs in biomedicine*, 187, 105243. <https://doi.org/10.1016/j.cmpb.2019.105243>
- Sánchez-Saquín, C. H., Soto-Cajiga, J. A., Barrera-Fernández, J. M., Gómez-Hernández, A., & Rodríguez-Olivares, N. A. (2025). Identification, Control, and Characterization of Peristaltic Pumps in Hemodialysis Machines. *Applied System Innovation*, 8(2), 44. <https://doi.org/10.3390/asi8020044>
- Santana, A., Neto, M., & Morales, R. (2020). Pressure Drop of Horizontal Air–Water Slug Flow in Different Configurations of Corrugated Pipes. *Journal of Fluids Engineering-transactions of The Asme*, 142(11): 111401. <https://doi.org/10.1115/1.4047676>
- Shin, H. C., Rohini, A. K., Kim, S. H., & Kim, S. M. (2024). An experimental study on pressure drop of air-oil flow in horizontal pipes using two synthetic oils. *International Journal of Mechanical Sciences*, 268, 108970. <https://doi.org/10.1016/j.ijmecsci.2024.108970>
- Sönmez, F. (2021). Koroner damarların farklı daralma geometrilerine bağlı olarak hemodinamik açıdan deneysel ve sayısal incelenmesi. Doktora tezi, Atatürk Üniversitesi, Fen Bilimleri Enstitüsü, Erzurum, Türkiye.
- Sönmez, F., Karagoz, S., Yıldırım, O., & Firat, I. (2023). Experimental and numerical investigation of the stenosed coronary artery taken from the clinical setting and modeled in terms of hemodynamics. *International Journal for Numerical Methods in Biomedical Engineering*, 40(1), e3793. <https://doi.org/10.1002/cnm.3793>
- Spencer, M. P., & Reid, J. M. (1979). Quantitation of carotid stenosis with continuous-wave (C-W) Doppler ultrasound. *Stroke*, 10(3), 326–330. <https://doi.org/10.1161/01.str.10.3.326>
- Stefanadis, C., Dernellis, J., Tsiamis, E., Stratos, C., Kallikazaros, I., & Toutouzas, P. (1998). Aortic function in patients during intra-aortic balloon pumping determined by the pressure-diameter relation. *The Journal of Thoracic and Cardiovascular Surgery*, 116(6), 1052–1059. [https://doi.org/10.1016/S0022-5223\(98\)70058-3](https://doi.org/10.1016/S0022-5223(98)70058-3)

- Stelios, S., Qin, S., Shan, F., & Mathioulakis, D. (2019). Forced and unforced flow through compliant tubes. *Meccanica*, 54(6), 779-798. <https://doi.org/10.1007/s11012-019-01002-6>
- Takagi, D., & Balmforth, N. J. (2011). Peristaltic pumping of viscous fluid in an elastic tube. *Journal of Fluid Mechanics*, 672, 196–218. <https://doi.org/10.1017/S0022112010005914>
- Tauber, F.J., Masselter, T., Speck, T. (2021). Biomimetic Soft Robotic Peristaltic Pumping System for Coolant Liquid Transport. In: Dröder, K., Vietor, T. (eds) *Technologies for economic and functional lightweight design. Zukunftstechnologien für den multifunktionalen Leichtbau*. Springer Vieweg, Berlin, Heidelberg. https://doi.org/10.1007/978-3-662-62924-6_14
- Verde, W.M., Biazussi, J.L., Estrada, C.P., Estevam, V., Tavares, A., Neto, S.J.A., Rocha, P.S.D.M.V. and Bannwart, A.C., 2021. Experimental investigation of pressure drop in failed Electrical Submersible Pump (ESP) under liquid single-phase and gas-liquid twophase flow. *Journal of Petroleum Science and Engineering*, 198, 108127. <https://doi.org/10.1016/j.petrol.2020.108127>
- Xie, J., Shih, J., Lin, Q., Yang, B., & Tai, Y. (2004). Surface micromachined electrostatically actuated micro peristaltic pump. *Lab on a chip*, 4 (5), 495-501. <https://doi.org/10.1039/B403906H>
- Yıldırım, O. (2023). Koroner arterlerde kan akışının çok fazlı etkilerinin deneysel ve sayısal olarak incelenmesi. Atatürk Üniversitesi, Fen Bilimleri Enstitüsü, Makine Mühendisliği Anabilim Dalı, Termodinamik Bilim Dalı. Doktora Tezi, Erzurum, TÜRKİYE.